Ambiguities in input-output behavior of driven nonlinear systems close to bifurcation

MARCO REIT, MICHAEL BERENS, WOLFGANG MATHIS

Leibniz Universität Hannover
Institute of Theoretical Electrical Engineering
Appelstraße 9A, 30167 Hannover, Germany
e-mail: reit@tet.uni-hannover.de

Abstract: Since the so-called Hopf-type amplifier has become an established element in the modeling of the mammalian hearing organ, it also gets attention in the design of nonlinear amplifiers for technical applications. Due to its pure sinusoidal response to a sinusoidal input signal, the amplifier based on the normal form of the Andronov-Hopf bifurcation is a peculiar exception of nonlinear amplifiers. This feature allows an exact mathematical formulation of the input-output characteristic and thus deeper insights of the nonlinear behavior. Aside from the Hopf-type amplifier we investigate an extension of the Hopf system with focus on ambiguities, especially the separation of solution sets, and double hysteresis behavior in the input-output characteristic. Our results are validated by a DSP implementation.

Key words: Andronov-Hopf, bifurcation, nonlinear amplifier, ambiguities

1. Introduction

In engineering, the modeling of a desired functionality to reproduce a certain biological or physical behavior is a common task. Usually a mathematical model serves as the basis to develop, for instance an electronic device. In the formulation of the mathematical description the accuracy of the modeling must be balanced against the simplicity of the equations. The latter also includes the computability of simulations and the feasibility of hardware implementations. Thus, the modeling process presupposes a comprehensive knowledge about suitable equations and their parameter dependencies to derive an equation with certain behavior. As a biological example, experimental data reveals that the active amplification process of the cochlea, the hearing organ in the mammalian auditory system, shows a compressive non-linearity with a universal 1/3-power law [1]. Besides this amplification characteristic, the cochlea exhibits also a sharper tuning for weaker input stimuli [1, 2]. To describe these biological features, the (truncated) normal form equation of the Andronov-Hopf bifurcation endowed with an excitation was proposed [3] and is widely used as basis element for several models of the auditory system [4-7]. To achieve the nonlinear amplification characteristic, the Hopf system is tuned close to the onset of the self-sustained limit cycle oscillation [3, 4].

Despite the nonlinearity of the so called Hopf-type amplifier, the study of the response characteristic has exposed, that a sinusoidal input signal leads to a pure sinusoidal output signal with the same frequency and without any harmonic distortions [3-9]. That means, apart from the specific nonlinear amplification characteristic, this Hopf-type amplifier acts on single-tone excitations like a linear system concerning the spectral behavior [8, 9]. This feature allows the calculation of an algebraic equation describing the input-output behavior in dependency of all given parameters [8, 9]. This is a common task in control systems engineering for linear time-invariant systems by means of amplitude-frequency and phase-frequency characteristics. Since nonlinear systems show harmonic distortions for single tone excitations, it is in general not possible to describe the input-output behavior with an algebraic equation. Hence, the sinus-to-sinus input-output behavior of this specific class of nonlinear amplifiers is greatly helpful to understand the parameter dependencies of the steady-state solution. Furthermore, it is obvious to use this feature in a constructive way to formulate bifurcation-based amplifiers with desired nonlinear input-output characteristics. To get closer to this objective, we investigate in this paper all parameter dependencies of the Hopf-type amplifier and consider an expansion of this system. Under certain conditions, we found ambiguities in form of hysteresis effects and separation of solution sets. The results and the applicability are verified by measurements of a DSP implementation.

2. Hopf-type amplifier

The Hopf-type amplifier is described by the (truncated) normal form equation of the Andronov-Hopf bifurcation with an additional excitation term. We use the ω_0 – rescaled form that is written as [4, 5, 9]

$$\dot{z} = (\mu + \mathrm{i})\omega_0 z + \sigma\omega_0 |z|^2 z - \omega_0 a(t), \tag{1}$$

with $z(t), a(t) \in \mathbb{C}$. Here, $\mu \in \mathbb{R}$ denotes the bifurcation parameter, i is the imaginary unit and ω_0 is the natural frequency of the oscillation. In general, the coefficient is a complex quantity defined by $\sigma = \sigma_R + \mathrm{i}\sigma_I$ substituting the external excitation $a(t) = p(t) + \mathrm{i}q(t)$ and the solution $z(t) = x(t) + \mathrm{i}y(t)$ in (1) results in the real representation of the Hopf amplifier

$$\begin{aligned} \dot{x} &= -\omega_0 y + \mu\omega_0 x + \omega_0(\sigma_R x - \sigma_I y)(x^2 + y^2) - \omega_0 p(t) \\ \dot{y} &= \omega_0 x + \mu\omega_0 y + \omega_0(\sigma_R y + \sigma_I x)(x^2 + y^2) - \omega_0 q(t) \end{aligned}, \tag{2}$$

where $q(t)$ denotes the Hilbert transform of $p(t)$. For a more accessible representation, the substitution $x = r\cos\varphi$ and $y = r\sin\varphi$ converts the system, neglecting the excitation, into polar coordinates

$$\begin{aligned} \dot{r} &= \omega_0 r(\mu + \sigma_R r^2) \\ \dot{\varphi} &= \omega_0 + \sigma_I \omega_0 r^2. \end{aligned} \tag{3}$$

The latter shows that the imaginary part of the coefficient σ affects only the frequency $\omega = \dot{\varphi}$ of the self-sustained oscillation. The steady-state solution without excitation is easily calculable from (3) and is shown in Fig. 1 for $\sigma_R = -1$ and $\sigma_I = 0$ together with the corresponding vector fields computed by (2) with $p(t) = q(t) = 0$.
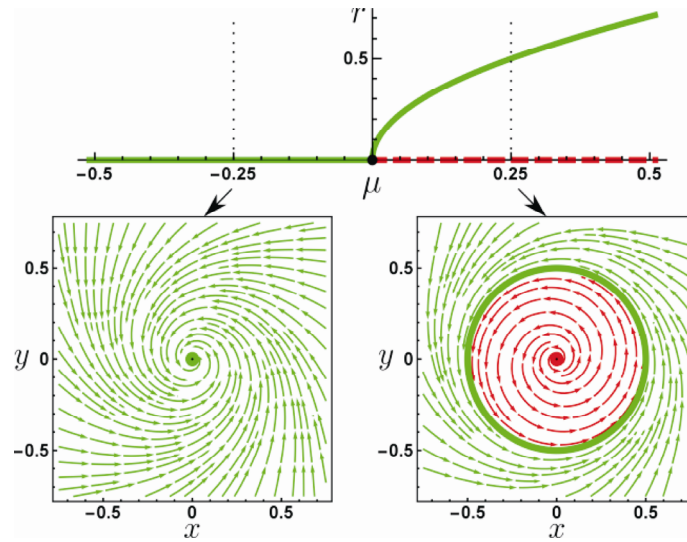

Fig. 1. Steady-state solutions of (3) with corresponding vector fields

For the operation as an amplifier, the Hopf system is only suitable in that region, where the two dimensional vector field exhibits only one stable fixed point. This condition is fulfilled when $\sigma_R < 0$ and $\mu \leq 0$ are both valid. Since the transition between the stable fixed point and the stable limit cycle occurs at $\mu = 0$ and the radius of the limit cycle grows by increasing the μ-value, the bifurcation is named supercritical [10]. In contrast, the system exhibits for $\sigma_R > 0$ a stable fixed point encircled by an unstable limit cycle for $\mu < 0$ and an unstable fixed point for $\mu \geq 0$. This kind of bifurcation is called subcritical [10]. Furthermore, the description of the Hopf system in polar coordinates (3) shows rotational symmetry around the fixed point (cf. Fig. 1). This behavior allows the assumption that the sinusoidal input signal $a(t) = a_0 e^{i\omega t}$ leads to the sinusoidal steady-state response $z(t) = z_0 e^{i(\omega t + \phi)}$. By substituting these signals in (1), this particular feature enables the calculation of algebraic Equations [3-5] that describe the input-output amplitude relation

$$a_0 = \sqrt{\left(\mu z_0 + \sigma_R z_0^3\right)^2 + \left(\left(1 - \frac{\omega}{\omega_0}\right)z_0 + \sigma_I z_0^3\right)^2}, \tag{4}$$

as well as the phase relation

$$\tan\phi = \frac{1 - \frac{\omega}{\omega_0} + \sigma_I z_0^2}{\mu + \sigma_R z_0^2}. \tag{5}$$

For modeling the mammalian auditory system, it is a common task to analyze (4) with the values $\sigma_R = -1$ and $\sigma_I = 0$. These settings lead to the steady-state response illustrated in Fig. 2.
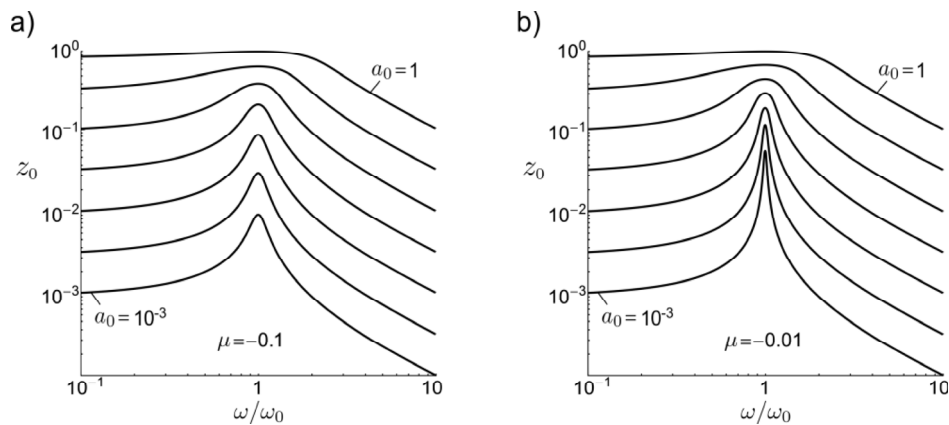

Fig. 2. Steady-state response of the Hopf-type amplifier

The stimulation strength, starting at $a_0 = 1$ with the upper curve, is decreased in steps of 10 dB. The input-output behavior shows a strong amplification of faint input signals with a sharper resonance for a smaller distance to the bifurcation point. This is one of the main effects a cochlea model has to exhibit [1-7]. In resonance ($\omega = \omega_0$) and with a tuning of the system into the bifurcation point ($\mu = 0$) the input-output amplitude relation $z_0 = a_0^{1/3}$ enables the modeling of the nonlinear dynamic compression revealed by physiological measurements [1-5].

3. Parameter dependencies and ambiguities

With the aim of a design concept for bifurcation-based amplifiers with a desired nonlinear input-output characteristic in a certain frequency band, it is necessary to understand all parameter dependencies of such a system. For the Hopf-type amplifier, the dependencies of the response regarding the nonlinearity parameter μ as well as the amplitude a_0 and the frequency ω of the excitation are well studied [3-6]. The influence of the imaginary part σ_I on the steady-state response of the Hopf-type amplifier is much less taken into account for modeling or general investigations [7, 9, 10]. In this paper we focus on the parameter dependencies of the complex coefficient σ of the nonlinear term in the driven normal form equation of the Andronov-Hopf bifurcation (1). Since σ is a complex quantity, it can be expressed beside the real and imaginary part by the absolute value $\hat{\sigma}$ and the phase θ that gives $\sigma = \sigma_R + i\sigma_I = \hat{\sigma}e^{i\theta}$. For all following investigations, we set the forcing amplitude to $a_0 = 0.1$. With the advantage of the exact description of the input-output amplitude relation in (4), we can investigate the resulting effects on the steady-state response caused by variation

of $\hat{\sigma}$ and θ. Therefore, we substitute $\sigma_R = \hat{\sigma}\cos\theta$ and $\sigma_I = \hat{\sigma}\sin\theta$ in (4). The results of the parameter study are shown in Fig. 3-5.
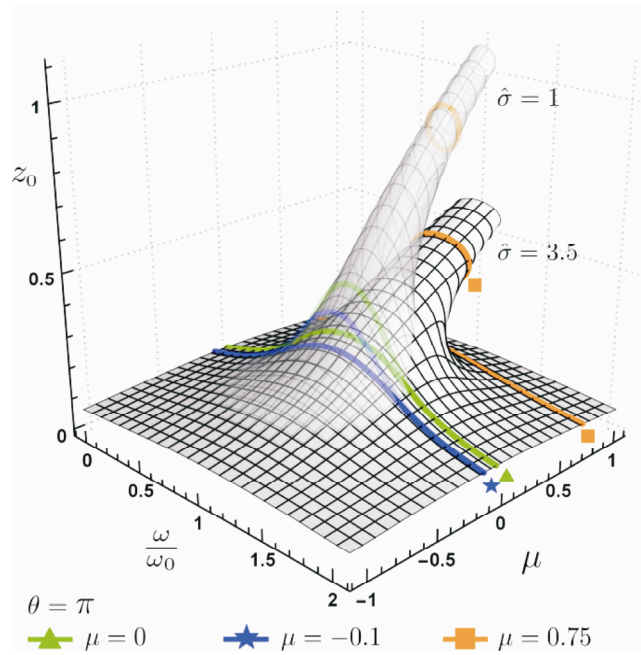

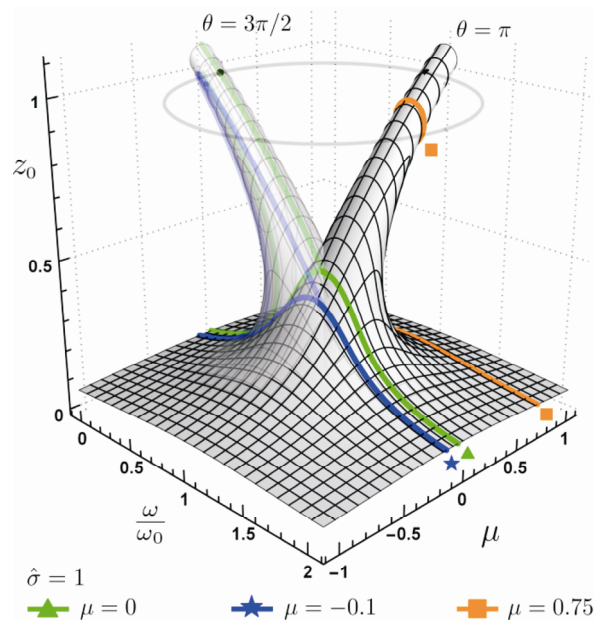Fig. 3. Parameter dependent output amplitude in variation of $\hat{\sigma}$

Fig. 4. Parameter dependent output amplitude in variation of θ
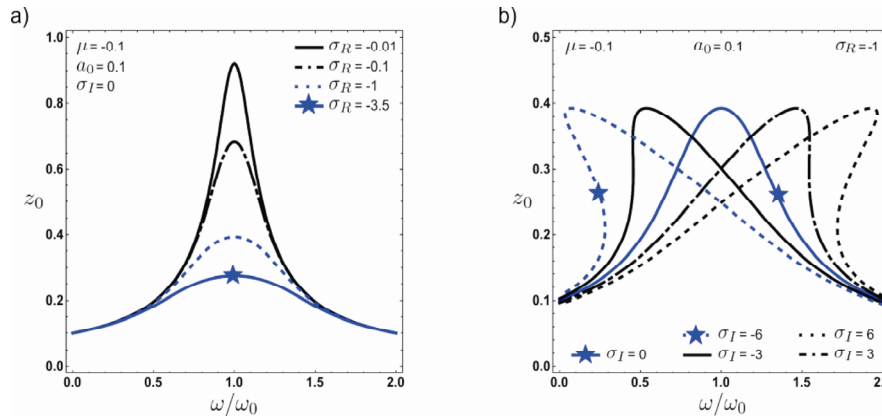
Fig. 5. Steady-state response: a) Variation of σ_R b) Variation of σ_I

In the first two figures we use a three-dimensional visualization, which gives a deeper understanding of the coherences between the given parameters. Additionally, the cross sections at $\mu = -0.1$, $\mu = 0$ and $\mu = 0.75$ are marked by solid lines. Since, the variation of $\hat{\sigma}$ towards higher values, pictured in Fig. 3, shows an uniform compression in the output amplitude z_0, $\hat{\sigma}$ denotes a damping factor. This behavior is also given by increasing σ_R for a fixed $\sigma_I = 0$, represented in Fig. 5a. The variation of θ causes a uniform rotation around the point $(\omega/\omega_0 = 1; \mu = 0)$ with a mathematically negative sense of direction. That means, the system shows the supercritical Andronov-Hopf bifurcation for an interval of $\pi/2 < \theta < 3\pi/2$. As shown in Fig. 4 at the cross section $\mu = -0.1$ the variation of θ leads for a fixed μ-value to a frequency shift of the resonance peak as well as an increase of the maximum. At a specific value of θ ambiguities occur, which cause hysteresis effects in the input-output amplitude relation. In contrast, if only the imaginary part σ_I is varied, the maximum value of the resonance peak remains unchanged (cf. Fig. 5b). For a constant negative σ_R the peak bends for $\sigma_I < 0$ towards lower and for $\sigma_I > 0$ towards higher frequencies (cf. Fig. 5b). Here, hysteresis effects arise for a certain relation between σ_R and σ_I [11]. The circular rotation of the whole resonance structure by varying θ can be proved by substituting $\omega = \omega_0 + \Omega\omega_0$ in (4) to shift the axis of rotation into the origin. We assume a specific output amplitude z_0 which rotates on a circle with the radius ρ in a mathematically negative sense of direction by varying $\theta \in [0, 2\pi]$. Thus, for each z_0 the corresponding parameter set can be described by $\mu = -\rho\cos(\theta+\alpha)$ and $\Omega = \rho\sin(\theta+\alpha)$ where each $\mu - \Omega$ μ-Ω-position is described by the radius ρ and the angle $\alpha \in [0, 2\pi]$ for a constant θ. The substitution of μ and Ω in the modified version of (4) leads to

$$a_0 = z_0\sqrt{\rho^2 - 2\hat{\sigma}\rho\,\cos(\alpha)z_0^2 + \hat{\sigma}^2 z_0^4}\ . \tag{6}$$

Due to the independency of (6) from θ it is clear that a constant input amplitude a_0 as well as constant parameters ρ, α and $\hat{\sigma}$ give a constant output amplitude z_0 on the assumed circle

with the radius ρ and the angle $\theta \in [0, 2\pi]$. This proves the circular rotation of the whole resonance structure by varying θ.

It is obvious that the Hopf-type amplifier can show ambiguities in the form of hysteresis behavior. But in the valid region of operation as amplifier, it is impossible to exhibit ambiguities in the form of separated solution sets as visible eg. in Fig. 3 for the marked cross section $\mu = 0.75$.

4. Expanded Hopf-type amplifier

Since the input-output behavior of the Hopf-type amplifier is fully understood, we expand the driven normal form equation of the Andronov-Hopf bifurcation (1) with a rotationally symmetric nonlinear term, which leads to the equation

$$\dot{z} = (\mu + \mathrm{i})\omega_0 z + \sigma\omega_0 |z|^2 z + \delta\omega_0 |z|^4 z - \omega_0 a(t) \,, \tag{7}$$

with $\delta = \delta_R + \mathrm{i}\delta_I$. To investigate the behavior of this system, we omit the excitation and convert (7) into polar coordinates

$$\begin{aligned} \dot{r} &= \omega_0 r(\mu + \sigma_R r^2 + \delta_R r^4) \\ \dot{\varphi} &= \omega_0 (1 + \sigma_I r^2 + \delta_I r^4) \end{aligned} \tag{8}$$

It is obvious, that similar to σ, the real part of δ affects the radius of the limit cycles, while the imaginary part influences the frequency of the self-sustained oscillation. The order of nonlinearity promises a more complicated system. Before studying the input-output behavior, it is necessary to determine that region, where the system exhibits only one stable fixed point and is therefore suitable as a nonlinear amplifier. The steady-state solutions of (8) are depicted in Fig. 6 for the parameters $\sigma_R = 1$, $\delta_R = -1$ and $\sigma_I = \delta_I = 0$.
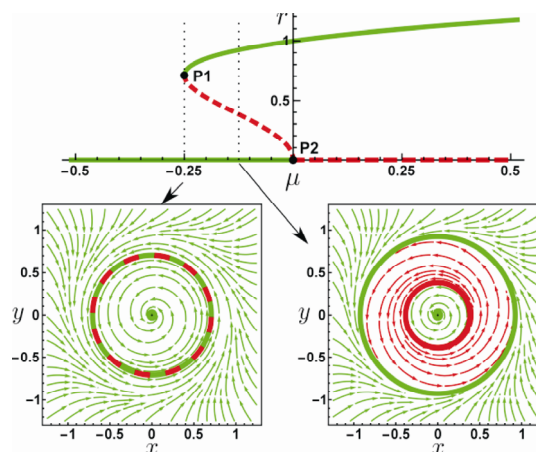

Fig. 6. Steady-state solutions of (8) with corresponding vector fields,
P1 – fold limit cycle bifurcation, P2 – Andronov-Hopf bifurcation

The corresponding vector fields in Fig. 6 are calculated by the real representation of (8) given by

$$\dot{x} = -\omega_0 y + \mu\omega_0 x - \omega_0 x\left(x^2 + y^2\right)\left(x^2 + y^2 - 1\right)$$
$$\dot{y} = \omega_0 x + \mu\omega_0 y - \omega_0 y\left(x^2 + y^2\right)\left(x^2 + y^2 - 1\right) \qquad (9)$$

A different kind of bifurcation scenario is observable. The range for μ that ensures the stable fixed point as the only steady-state solution, is calculable to $\mu < -0.25$. At the point $\mu = -0.25$ a limit cycle arises, which acts as attractor for the vector field outside of the circle. For the inside vector field, the circle acts repellent and the fixed point is attracting. This is the bifurcation point of the so-called fold limit cycle bifurcation [10]. This limit cycle splits for $\mu > -0.25$ into a stable outer limit cycle and an unstable inner limit cycle. At the point of the subcritical Andronov-Hopf bifurcation ($\mu = 0, \sigma_R > 0$) the unstable limit cycle disappears.
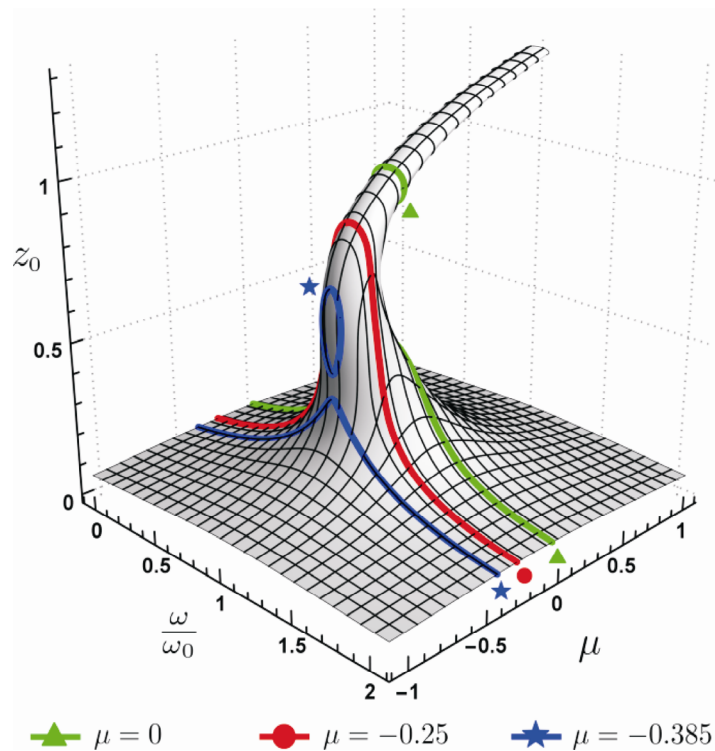

Fig. 7. Parameter dependent output amplitude of (7), $\sigma = 1$, $\sigma = -1$

However, since the system is rotationally symmetric, the input-output behavior is still precisely predictable by an algebraic equation. Substituting, equivalent to the standard Hopf-type amplifier in section 2, the assumed sinusoidal input and output signals in (7), the input-output amplitude relation is given by

$$a_0 = \sqrt{(\mu z_0 + \sigma_R z_0^3 + \delta_R z_0^5)^2 + \left(\left(1 - \frac{\omega}{\omega_0}\right)z_0 + \sigma_I z_0^3 + \delta_I z_0^5\right)^2}. \tag{10}$$

For first investigations of the behavior of the expanded system, we set the input amplitude to $\alpha_0 = 0.1$ and the coefficients to $\sigma_R = 1$, $\delta_R = -1$ and $\sigma_I = \delta_I = 0$. The resulting input-output characteristic is shown in Fig. 7. It must be kept in mind that $\mu < -0.25$ denotes the valid region for the system to act as an amplifier. In contrast to the standard Hopf-type amplifier, it is obvious that this system exhibits separated solution sets in a small region of μ (cf. Fig. 7 $\mu = -0.385$). Since the imaginary parts of the coefficients σ and δ are set to zero, no rotation or bending towards lower or higher frequencies appears. To investigate the separated solution sets, the real representation of the expanded system (9) endowed with an excitation (cf. (2)) is implemented on a digital signal processor and solved by 4th-order Runge-Kutta method [5].
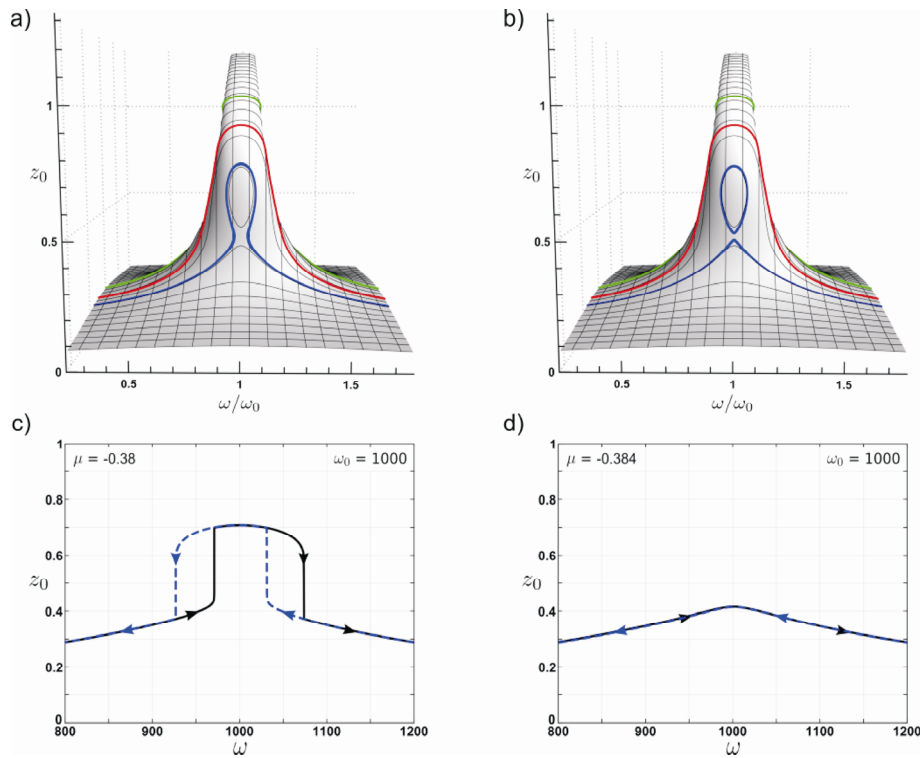

Fig. 8. Steady-state response of the expanded system (7), $\sigma = 1$, $\delta = -1$; a), b) calculation results of (10); c), d) measurement results of the DSP-implementation

The measurement results are shown in Fig. 8c and 8d while the nonlinearity parameter μ serves as control parameter. For instance the calculated input-output characteristic given by (10) reveals for $\mu = -0.38$ a double hysteresis behavior (cf. Fig. 8a). That means the maxi-

mum of the output signal depends on the direction of the frequency sweep. Both hysteresis loops are mirror-symmetric at the natural frequency $\omega_0 = 1000$. These results are validated by the measurements as depicted in Fig. 8c. The variation of μ towards lower values increases the hysteresis loops until the gap at the natural frequency is closed. Thus, the maximum of the output amplitude drops suddenly. This already occurs for $\mu = -0.384$, where ambiguities exist in form of a separated solution set (cf. Fig. 8b). The corresponding measurement results are depicted in Fig. 8d. It is clear, that the measurements cannot show the separated solutions by a frequency sweep. However, starting the measurement with an initial value of the separated solution, it can be verified, that this solutions are existent and stable.

It is obvious, that the input-output behavior can strongly be modified by varying the parameters σ and δ. For instance the input-output characteristic of (10) for $\sigma = 2$ and $\delta = -0.8$ as well as $a_0 = 0.1$ is shown in Fig. 9. Here, the valid region for the nonlinear parameter is $\mu < -1.25$ where the system always exhibits a separated solution set. We expect much complicate input-output behavior for $\sigma_I \neq 0$ and $\delta_I \neq 0$.
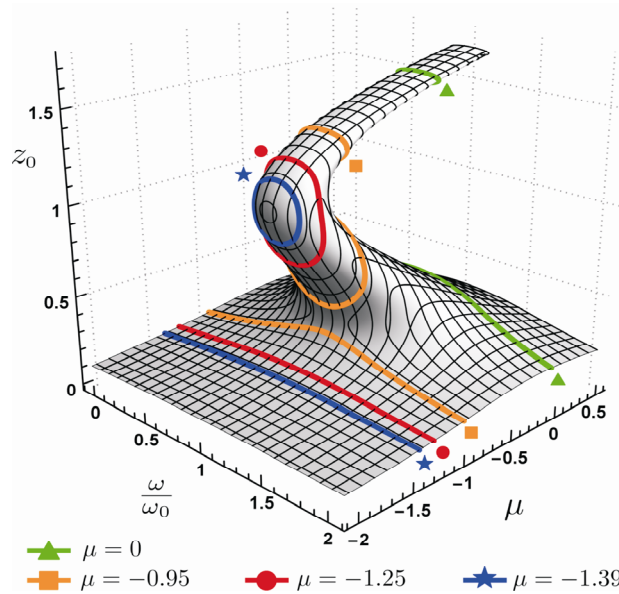

Fig. 9. Parameter dependent output amplitude of (10), $\sigma = 2$, $\delta = -0.8$

5. Conclusions

The Hopf-type amplifier shows an interesting nonlinear input-output behavior with strong amplification of faint signals within a narrow bandwidth. Hence, besides the modeling of the mammalian hearing organ, the Hopf amplifier gets attention for technical applications. The remarkable filtering characteristics promises new possibilities in engineering sciences e.g. in measurement systems or sensor applications. In this paper we investigate all parameter depen-

dencies of the Hopf-type amplifier to understand the complete input-output behavior. Furthermore, we study the input-output characteristic of an expanded version of this amplifier with focus on new features, especially ambiguities such as hysteresis or separated solution sets. We validate the results by implementation and measurements on a digital signal processor. Since the considered systems are rotationally symmetric, they response to a sinusoidal input signal with a pure sinusoidal output signal of the same frequency and without any harmonic distortions. This feature enables the calculation of algebraic equations which precisely describe the input-output amplitude and phase relations. This advantage is greatly helpful to get deeper insights of the parameter dependent behavior of the nonlinear amplifiers. On the one hand, the algebraic equations describe all possible solutions of the output, which might be not observable by measurements. On the other hand, with the deeper understanding of the input-output behavior, we get closer to a design concept for bifurcation-based amplifiers with a desired nonlinear input-output characteristic in a certain frequency band.

References

[1] Szalai R., Champneys A., Homer M., Maoileidigh D.O., Kennedy H., Cooper N., *On the origins of the compressive cochlear nonlinearity*, Working Paper (2011).

[2] Ruggero M.A., *Responses to sound of the basilar membrane of the mammalian cochlea*, Current Opinion in Neurobiology 2: 449-456 (1992).

[3] Eguíluz V.M., Ospeck M., Choe Y., Hudspeth A.J., Magnasco M.O., *Essential nonlinearities in hearing*, Physical Review Letters 84: 5232-5235 (2000).

[4] Stoop R., Jasa T., Uwate Y., Martignoli S., *From Hearing to Listening: Design and Properties of an Actively Tunable Electronic Hearing Sensor*, Sensors 7: 3287-3298 (2007).

[5] Reit M., Mathis W., Stoop R., *Time-Discrete Nonlinear Cochlea Model Implemented on DSP for Auditory Studies*, Proceedings of the 20th International Conference on Nonlinear Dynamics of Electronic Systems (NDES 2012).

[6] Camalet S., Duke T., Jülicher F., Prost J., *Auditory sensitivity provided by self-tuned critical oscillations of hair cells*, Proceedings of the National Academy of Sciences 97(7): 3183-3188 (2000).

[7] Montgomery K.A., Silber M., Solla S.A., *Amplification in the auditory periphery: the effect of coupled tuning mechanisms*, Physical Review E 75: 051924 (2007).

[8] Reit M., Stoop R., Mathis W., *Analysis of Cascaded Canonical Dissipative Systems and LTI Filter Sections*, Acta Technica 59(1): 79-96 (2014).

[9] Reit M., Mathis W., *A Class of Sinusoidal Driven Nonlinear Input-Output Systems with Sinusoidal Response*, International Symposium on Nonlinear Theory and its Applications (2014).

[10] Kuznetzov Y.A., *Elements of Applied Bifurcation Theory*, Springer (2004).

[11] Zhang Y., Golubitsky M., *Periodically Forced Hopf Bifurcation*, SIAM Journal on Applied Dynamical Systems 10(4): 1272-1306 (2011).